Journal of Physics: Conference Series

Coupled two-core integrated waveguides modal analysis

Coupled two-core integrated waveguides modal analysis

David Benedicto, M. Victoria Collados, Juan C. Martín, Jesús Atencia, Juan A. Vallés

Department of Applied Physics and I3A, Faculty of Sciences, University of Zaragoza, C/P. Cerbuna 12, 50009, Zaragoza, Spain

dbenedicto@unizar.es

Abstract. We present a modal analysis of coupled two-core integrated waveguides fabricated by femtosecond laser writing as a function of the core-to-core distance, illuminating position and input light wavelength. In order to do that we use the correlation filter method, implementing the computer generated holograms in a phase-only spatial light modulator. Due to the two-core waveguide symmetry, we prove it is not necessary to encode the complex amplitude in a phase-only device as long as the cores are not strongly coupled. A comparison between experimental and numerical modal weights is presented, showing that simple phase-only match filters allow the modal decomposition of two-core waveguides output beams.

1. Introduction

Formation of 3D micro-structures with a wide range of geometries and configuration has been possible thanks to recent advances on strongly focused femtosecond laser pulses direct writing technique [1]–[4], which has a potential significant impact on a varied range of applications [5]–[7]. Thanks to this technique, integrated multicore structures with almost unlimited geometries can be fabricated, thus allowing the transfer of multicore fiber designs potentialities to integrated structures.

Multicore fibers (MCF) are currently of great interest in optical communications due to their suitability for increasing the capacity of optical fibers through modal and space division multiplexing [8], their designs possibilities for large mode area fibers particularly useful for high-power fiber amplifiers and laser [9] and their core-coupling sensitivity to external conditions that allows the fabrication of interferometer-like optical fiber sensors [10].

With the development of integrated multicore structures, the knowledge and control of the modes propagated by these waveguides has acquired a great importance, and the characterization of optical fields by means of mode decomposition (MD) results in a key factor for the analysis, design and optimization of integrated optical devices based on these structures, specially due to their high number of degrees of freedom (i.e. arrangements, pitch, size and number of individual cores). On the one hand, mode division multiplexing requires encoding and de-coding of the information carried in the supermode of the structure, for which a technique for the excitation and decomposition of such modes is essential. On the other hand, the complexity of multi-supermode lasing and modal competition makes this tool fundamental in order to study multicore gain. Moreover, during the propagation of light along the fiber, multiple effects (mode mixing, modal phase delays, modal bend loss, etc.) could take place. The MD is also a key tool in order to study these transmission disturbances.

There are different approaches to perform a MD, basically divided into numerical routines (e.g. GS algorithm [11], SPGD algorithm [12]. genetic algorithm [13]) and experimental methods (e.g. ring resonators [14], multimode interference [15], low-coherence interferometry [16], correlation filter method [17]). Among the different MD techniques, we focus on the correlation filter methods (CFM), that allows us to perform a real-time modal analysis by implementing computer generated holograms (CGH) into a spatial light modulator (SLM). Despite this method has shown excellent results for fiber MD [18]–[21], a complete analysis of the modal distribution at the output of multicore integrated waveguides, which is essential to fully characterize the modal distribution propagating by the guiding structure, has not yet been performed using this type of device.

In this work we present the modal analysis of coupled two-core integrated waveguides fabricated in a phospate glass by femtosecond laser writing. The previous characterization of this set of waveguides can be found in [22].

2. Correlation filter method modal analysis

The notation to be employed is established in Figure 1, which shows a basic scheme of the setup necessary for MD. The two-core waveguide output field to be analyzed, $U(\eta,\xi)$, constitutes the input CGH field. The input electric field after going through the beam expansor, $U(x,y)$, the CGH transmittance, $T(x,y)$, and the output distribution, $W(u,v)$, at the L_3 lens focal plane are related by [23]

$$W(u,v)=\frac{1}{i\lambda f}\mathcal{F}[U(x,y)\cdot T(x,y)], \tag{1}$$

where $\mathcal{F}$ denotes Fourier transform, $i=\sqrt{-1}$, λ is the input light wavelength, f is the L_3 lens focal distance and the coordinates at the focal plane (u,v) are related to the Fourier transform frequency space coordinates f_x and f_y by means of $u=\lambda f f_x$, $v=\lambda f f_y$.

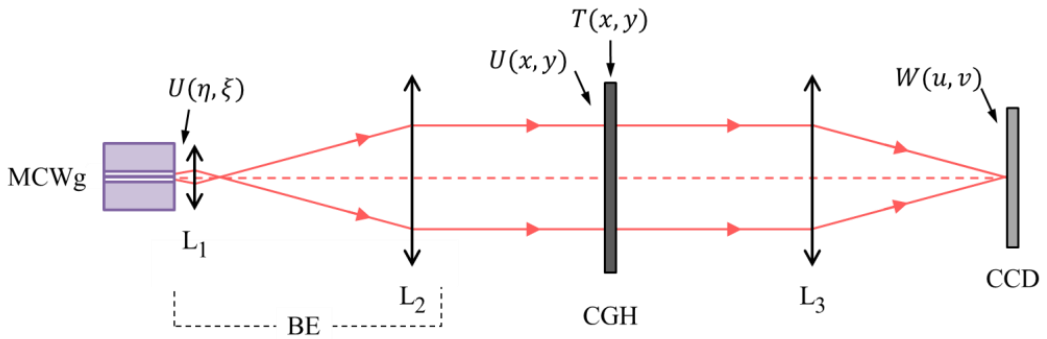

Figure 1 Experimental setup for MD. MCWg: multicore waveguide. BE: beam expansor. L_1, L_2 and L_3 are lenses, CGH: computer generated hologram, CCD: camera.

When the isolated cores of the multicore structure are single mode, the multicore waveguide has the same number of supermodes than cores [24]. Thus, the transverse optical field at the two-core waveguide output end can be expressed as

$$U(\eta,\xi)=c_s\varphi_s(\eta,\xi)+c_a\varphi_a(\eta,\xi), \tag{2}$$

being (η,ξ) the spatial coordinates at the waveguide output end, φ_m the symmetric (m=s) and antisymmetric (m=a) supermodes, and $c_m=\rho_m e^{i\theta_m}$ their complex expansion coefficients with amplitude ρ_m and phase θ_m. By using the coupled mode theory (CMT), one can write the supermodes as a function of the modes of the individual cores $(\varphi_n, n=1,2)$. When both of them are identical, and in weakly coupling regime, the expression is as follows [25]:

$$\varphi_m(\eta,\xi)=\frac{1}{\sqrt{2}}[\varphi_1(\eta,\xi)\pm\varphi_2(\eta,\xi)]. \tag{3}$$

in which the + sign accounts for the symmetric supermode and the – sign for the antisymmetric one.

The main task of the modal analysis is to determine the modal amplitude, ρ_m, of the supermodes propagating along the waveguide. To do so, we employ the CFM [17], in which a CGH with transmission

$$T(x,y) = \varphi_l^*(x,y), \tag{4}$$

is placed in the front focal plane of a lens, whose coordinates are given by (x,y), so that in the back focal plane the signal on the optical axis is proportional to the power guided by the respective mode [17]: $|\rho_l|^2$ in our case.

Regarding Eq. 3, one can see that the supermodes distributions need to be calculated before the experiment in order to perform the modal analysis. As the CGH is going to be implemented in a phase-only SLM, it is necessary to encode the complex amplitude in a phase only device, for which several techniques are known [26]–[29]. However, taking advantage of the special symmetry of the two-core waveguides with identical cores, in this work it will not be necessary using any of these techniques.

We assume single mode isolated cores, and suppose the modes (φ_n with n=1,2) to fulfill a series of properties. As we are in weakly guiding regime, with enough core-to-core separation, we assume the overlap between both functions to be negligible:

$$\langle\varphi_1|\varphi_2\rangle = \int_{\eta=-\infty}^{+\infty}\int_{\xi=-\infty}^{+\infty}\varphi_1(\eta,\xi)\varphi_2^*(\eta,\xi)d\eta d\xi = 0 \tag{5}$$

Note this is not due to orthogonality, as it happens with the supermodes product: $\langle\varphi_s|\varphi_a\rangle = 0$. We also consider our origin $(\eta = 0)$ to be between both functions, φ_1 being at the left $(\eta < 0)$ and φ_2 at the right $(\eta > 0)$ regarding the η axis. In the case of a step index waveguide, the fundamental mode has some symmetry properties. The following approach is valid as long as

$$\varphi_2(\eta,\xi) = \varphi_1(-\eta,-\xi). \tag{6}$$

This property has some consequences on the parity of both the symmetric and antisymmetric supermodes. Taking into account Eqs. (3) and (6), the symmetric mode has even parity, while the antisymmetric one has odd parity. All these properties are easy to see in the Fig. 2, where we have used a Gaussian-like profile as a mode function.

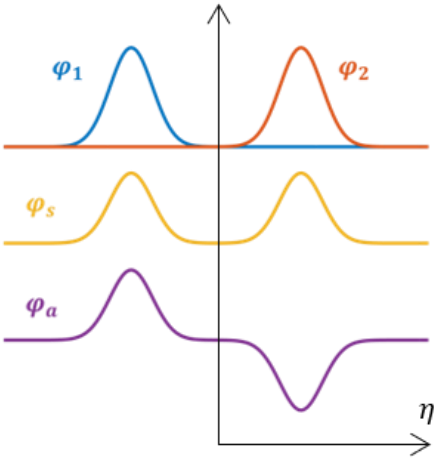

Figure 2 Schematic representation of the $\boldsymbol{\varphi_1}$, $\boldsymbol{\varphi_2}$, $\boldsymbol{\varphi_s}$ and $\boldsymbol{\varphi_a}$ electric field amplitude profiles along the $\boldsymbol{\eta}$-axis.

Our SLM allows us to implement phase-only CGH. As a consequence, it is necessary to draw upon some technique to encode a complex transmittance in a phase-only device. However, in this work we hypothesize that it is possible to perform the MD with phase-only correlation filters. Fig. 3. shows these filters, $\omega_m(x,y)$, together with the supermodes distribution. The symmetric filter consists in a constant phase (i.e. 0), while the antisymmetric has a phase jump of π (i.e. 0 and π) between its left and right sides (now related to the x-axis due to being at the CGH plane).

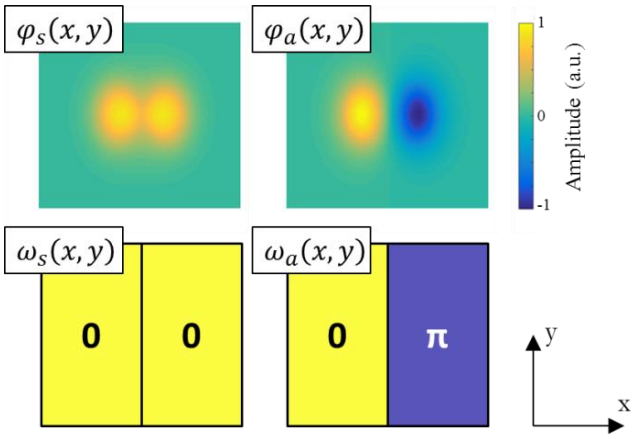

Figure 3 Proposed phase-only correlation filters, $\boldsymbol{\omega_m(x,y)}$, together with its transversal electric field distributions, $\boldsymbol{\varphi_m(x,y)}$.

The advantages of its use are clear: on one side, there is no need to use any technique to implement complex amplitudes in a phase-only device. On the other hand, the adjustment is much simpler. While if using the complex distribution one needs to center the CGH size and position, both in the x-axis and y-axis, the phase functions only need to be adjusted in the x-axis (the axis between cores).

In the CFM-MD, the electric field at the L_3 focal plane axis $(u = 0, v = 0)$, where the CCD is placed to measure the intensity, is proportional to the filtered mode content [17]:

$$W(u=0,v=0) \propto \sum_{m=1}^{2} c_m \iint_{-\infty}^{\infty} \varphi_m(x,y)\varphi_l^*(x,y)\,dxdy = \sum_{m=1}^{2} c_m \delta_{ml} = c_l, \qquad (7)$$

where φ_l is the l-th mode we are trying to detect and we have taken into account the orthonormality relationship between supermodes $\langle\varphi_m|\varphi_l\rangle = \delta_{ml}$.

However, as we no longer have a complex transmittance but a phase-only one, we are facing a slightly different problem. Instead of $\varphi_l^*(x,y)$ we have a function defined as:

$$f_l(x,y) = \mathrm{e}^{\omega_l(x,y)}, \qquad (8)$$

that in the case of our two-core waveguide is simplified as follows:

$$f_s(x,y) = 1 \quad \text{and} \quad f_a(x,y) = \begin{cases} 1, & \text{if } -\infty < x \leq 0 \\ -1, & \text{if } 0 < x < \infty \end{cases}. \qquad (9)$$

In order to perform the MD with a phase-only transmittance, the $f_l(x,y)$ function needs to satisfy the orthogonality property:

$$\int_{x=-\infty}^{+\infty}\int_{y=-\infty}^{+\infty} \varphi_m(x,y) f_l^*(x,y)dxdy \propto \delta_{ml}, \qquad (10)$$

which, in general, does not. Nevertheless, thanks to the special symmetry of the two core waveguides, this relationship is fulfilled. On one hand, both cross products are zero due to the functions parity:

$$\int_{x=-\infty}^{+\infty}\int_{y=-\infty}^{+\infty} \varphi_s(x,y) f_a^*(x,y)dxdy = 0 \qquad (11)$$

and

$$\int_{x=-\infty}^{+\infty}\int_{y=-\infty}^{+\infty} \varphi_a(x,y) f_s^*(x,y)dxdy = 0. \qquad (12)$$

The functions f_a^* and f_s^* are odd and even, respectively. They multiply, in each case, a function with the opposite parity. Thus, the products have odd symmetry and, as a consequence, its integral between symmetric limits is zero.

On the other hand, the same-mode-functions product gives the same result, thus fulfilling the orthogonality property. The antisymmetric supermode product can be expressed as a function of the individual core modes, due to its zero overlapping:

$$\begin{aligned}\int_{x=-\infty}^{+\infty}\int_{y=-\infty}^{+\infty}\varphi_a(x,y)f_a^*(x,y)dxdy \\ &= \int_{x=-\infty}^{0}\int_{y=-\infty}^{+\infty}\varphi_a(x,y)dxdy - \int_{x=0}^{+\infty}\int_{y=-\infty}^{+\infty}\varphi_a(x,y)dxdy \\ &= \frac{1}{\sqrt{2}}\left[\int_{x=-\infty}^{0}\int_{y=-\infty}^{+\infty}\varphi_1(x,y)dxdy + \int_{x=0}^{+\infty}\int_{y=-\infty}^{+\infty}\varphi_2(x,y)dxdy\right]dxdy \\ &= \int_{x=-\infty}^{+\infty}\int_{y=-\infty}^{+\infty}\varphi_s(x,y)dxdy.\end{aligned} \tag{13}$$

One can see that, by taking again into account the limits of the φ_1 and φ_2 functions, it gives the same result as the symmetric case:

$$\int_{x=-\infty}^{+\infty}\int_{y=-\infty}^{+\infty}\varphi_a(x,y)f_a^*(x,y)dxdy = \int_{x=-\infty}^{+\infty}\int_{y=-\infty}^{+\infty}\varphi_s(x,y)f_s^*(x,y)dxdy. \tag{14}$$

Eqs. 11, 12 and 14 describe an orthogonality relationship. This allows us to perform the modal analysis with a phase-only filter.

The validity of the previous approach depends on the coupling between the dual waveguide cores. If the cores are coupled enough, equation 5 is not satisfied and we cannot assume φ_1 and φ_2 to be restricted to the left and right sides along the η-axis, respectively. As this coupling depends on different parameters (i.e. core-to-core distance, wavelength, diameter and refractive index variation), we have performed a series of simulations taking into account our multicore waveguide, whose parameters can be consulted in Ref. [22]. As remarkable ones, the core diameter and refractive index variations of the waveguides are 5.3 μm and $6.3\cdot10^{-3}$, respectively. Taking into account the numerical results, we need to keep ourselves in core-to-core distances higher than 8 μm when illuminating at λ=1534 nm. Otherwise, the phase-only approach does not match the expected results.

3. Experimental setup

The required MD experimental setup is depicted in Fig. 4. An HI-1060 SMF illuminates the two-core waveguide (the light source being the tunable laser 8164B Lightwave Measurement System from Agilent Technologies, with a wavelength spectrum range from 1440 to 1630 nm, a spectral width under 1 nm and output power between 100 μW and 10 mW). In order to increase the effective resolution, the multicore output beam size is magnified at the SLM display using a microscope objective (DIN×40) and a lens (f_2=50 cm) following a 4f configuration. The 4f-lens combination images the two-core waveguide output beam through the beam splitter (BS) in the phase-only SLM operating in reflection mode (LUNA TELCO Phase Only Spatial Light Modulator from Holoeye [30], a full HD device with 1920×1080 square pixels with dimensions 4.5×4.5 μm^2, that modulates light in a wavelength range from 1400 nm to 1700 nm). As it only operates in the horizontal polarization, we select this state of polarization from the input beam with a linear polarizer (LP). The reflected field from the SLM, where the CGH is implemented, is Fourier transformed by lens L_3 (f_3=50 cm) and this signal is detected by the CCD camera (Bobcat-320 from Xenics, 900 to 1700 nm wavelength range, 320× 256 pixels with dimensions 20 × 20 μm^2), placed at the L_3 lens focal plane, where the modal weight is obtained. The SLM was previously calibrated following the procedure described in [31].

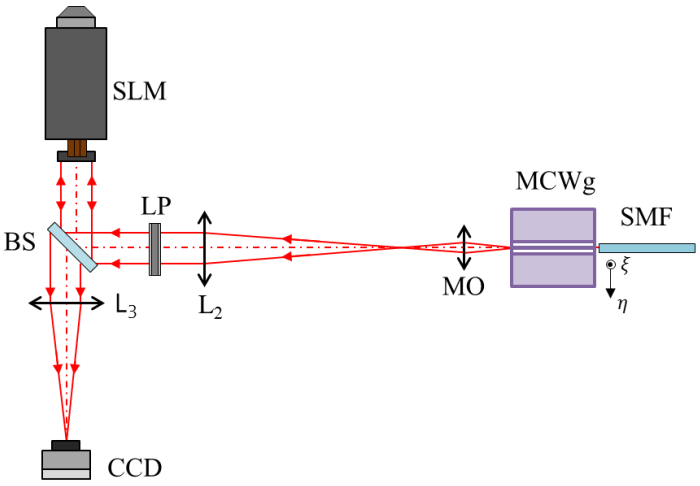

Figure 4 MD experimental setup. SLM: spatial light modulator, BS: beam splitter, LP: linear polarizer, L_2 and L_3 are lenses, MO: microscope objective, MCWg: multicore waveguide, SMF: single mode fiber, η and ξ orthogonal coordinates in the waveguide transversal plane.

4. Comparison between simulation and experimental results

Both the symmetric and antisymmetric modal weights of the two-core waveguide have been measured, following the CFM phase-only approximation presented in section 2, for two different core-to-core distances and as a function of the input fiber transversal position along the η-axis. At the same time, these modal weights have been numerically obtained by computing the projection of light from the SMF into the MCWg, its propagation along the two-core-fiber and, finally, simulating the modal decomposition of its output beam by the CFM. Fig. 5 shows the normalized modal weights as a function of the input fiber position for both the symmetric and antisymmetric supermodes for both a) 10 μm and b) 14 μm core-to-core distances. A good agreement between numerical and experimental values is shown in both cases, confirming the good performance of the phase-only CFM approach.

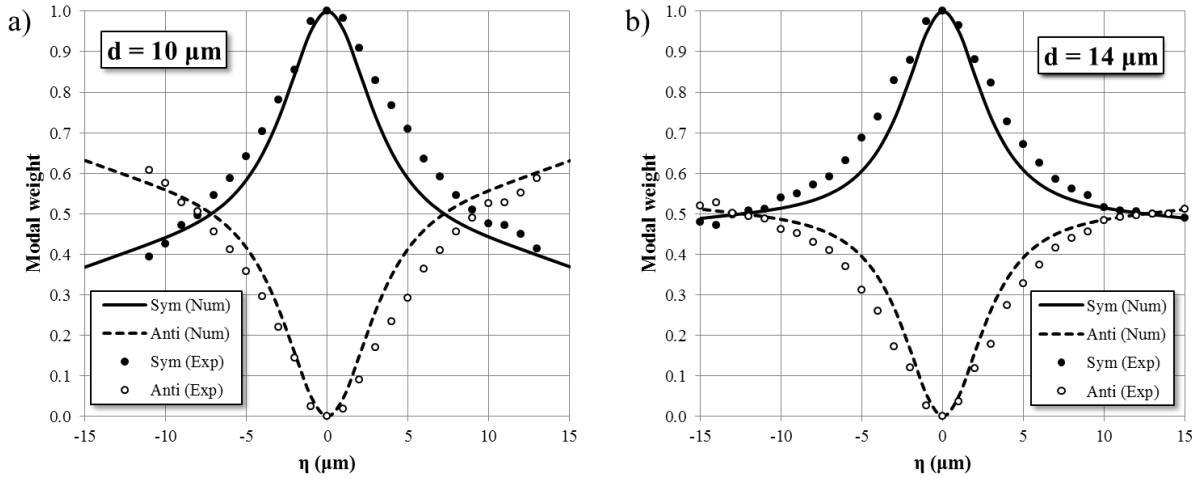

Figure 5 Comparison between numerical (Num) and experimental (Exp) normalized modal weights for both symmetric (Sim) and antisymmetric (Anti) supermodes as a function of the SMF excitation position along the η-axis, for a) 10 and b) 14 μm core-to-core distances (d). λ=1534 nm.

In the symmetric supermode case, its modal weight is maximized when the input fiber is placed between both cores. The antisymmetric supermode follows an opposite behavior, increasing its value as the input fiber moves away from the center, and reaching symmetric modal weight values when the input fiber position is further from the center than the cores itself.

In the 10 μm core-to-core distance two-core waveguide we have simulated and measured the modal weight evolution for two more different wavelengths: 1440 and 1630 nm. In order to do that, the SLM had to be recalibrated for each case. Fig. 6 a) and b) shows both cases, respectively. As the mode coupling depends on the wavelength, a variation between both cases can be seen. Again, in both of them a good agreement is shown between numerical and experimental modal weights, with a few exceptions of some points at the ends, owing to the small optical power coupled from the input fiber into the multicore waveguide.

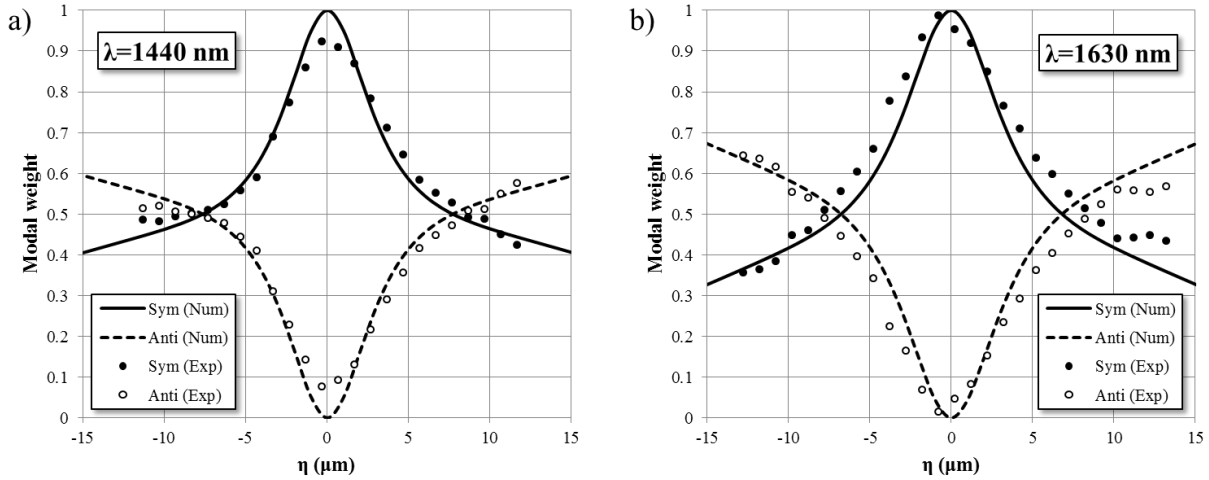

Figure 6 Comparison between numerical (Num) and experimental (Exp) normalized modal weights for both symmetric (Sim) and antisymmetric (Anti) supermodes as a function of the SMF excitation position along the η-axis, for the wavelengths a) 1440 and b) 1630 nm. 10 μm core-to-core distance.

5. Conclusion

A mode decomposition approach for weakly coupled two-core waveguides has been proposed. It consists on a simplification of the correlation filter method for which no complex amplitude encoding in phase-only devices is mandatory. The approach is analytically proved and numerically analyzed in order to study the range of application.

This technique has been experimentally tested by measuring the modal weights at two-core waveguides output ends as a function of the input fiber excitation position and for different coupling between cores by selecting two different core-to-core distances and three different wavelengths. A good agreement has been shown in all the cases, confirming the good performance of the phase-only CFM approach.

Moreover, despite the correlation filter method has been used several times in multimode fibers, it is, to our knowledge, the first time it is used to modally analyze a multicore integrated waveguide. The good results based on a twin core assumption also highlight the quality of the two-core integrated waveguides fabrication process by femtosecond laser writing.

References

[1] S. Gross and M. J. Withford, "Ultrafast-laser-inscribed 3D integrated photonics: challenges and emerging applications," *Nanophotonics*, vol. 4, no. 3, pp. 332–352, 2015.

[2] K. Sugioka, "Progress in ultrafast laser processing and future prospects," *Nanophotonics*, vol. 6, no. 2, pp. 393–413, 2017.

[3] T. T. Fernandez M. Sakadura, S. M Eaton, B. Sotillo, J. Siegel, J. Solis, Y. Shimotsuma, K. Miura, "Bespoke photonic devices using ultrafast laser driven ion migration in glasses," *Prog. Mater. Sci.*, vol. 94, pp. 68–113, 2018.

[4] J. Choi, M. Ramme, and M. Richardson, "Directly laser-written integrated photonics devices including diffractive optical elements," *Opt. Lasers Eng.*, vol. 83, pp. 66–70, 2016.

[5] D. Choudhury, J. R. Macdonald, and A. K. Kar, "Ultrafast laser inscription: perspectives on future integrated applications," *Laser Photon. Rev.*, vol. 8, no. 6, pp. 827–846, 2014.
[6] F. Sima, K. Sugioka, R. M. Vázquez, R. Osellame, L. Kelemen, and P. Ormos, "Three-dimensional femtosecond laser processing for lab-on-a-chip applications," *Nanophotonics*, vol. 7, no. 3, pp. 613–634, 2018.
[7] K. Sugioka and Y. Cheng, "Femtosecond laser three-dimensional micro-and nanofabrication," *Appl. Phys. Rev.*, vol. 1, no. 4, p. 41303, 2014.
[8] K. Saitoh and S. Matsuo, "Multicore fiber technology," *J. Light. Technol.*, vol. 34, no. 1, pp. 55–66, 2016.
[9] M. M. Vogel, M. Abdou-Ahmed, A. Voss, and T. Graf, "Very-large-mode-area, single-mode multicore fiber," *Opt. Lett.*, vol. 34, no. 18, pp. 2876–2878, 2009.
[10] J. Villatoro, O. Arrizabalaga, E. Antonio-Lopez, J. Zubia, and I. S. de Ocáriz, "Multicore fiber sensors," in *2017 Optical Fiber Communications Conference and Exhibition (OFC)*, pp. 1–3, 2017.
[11] R. W. Gerchberg, "A practical algorithm for the determination of plane from image and diffraction pictures," *Optik (Stuttg).*, vol. 35, no. 2, pp. 237–246, 1972.
[12] H. Lü, P. Zhou, X. Wang, and Z. Jiang, "Fast and accurate modal decomposition of multimode fiber based on stochastic parallel gradient descent algorithm," *Appl. Opt.*, vol. 52, no. 12, p. 2905, 2013.
[13] L. Li, J. Leng, P. Zhou, and J. Chen, "Multimode fiber modal decomposition based on hybrid genetic global optimization algorithm," *Opt. Express*, vol. 25, no. 17, pp. 19680–19690, 2017.
[14] N. Andermahr, T. Theeg, and C. Fallnich, "Novel approach for polarization-sensitive measurements of transverse modes in few-mode optical fibers," *Appl. Phys. B*, vol. 91, no. 2, p. 353, 2008.
[15] J. W. Nicholson, A. D. Yablon, S. Ramachandran, and S. Ghalmi, "Spatially and spectrally resolved imaging of modal content in large-mode-area fibers," *Opt. Express*, vol. 16, no. 10, p. 7233, 2008.
[16] Y. Z. Ma *et al.*, "Fiber-modes and fiber-anisotropy characterization using low-coherence interferometry," *Appl. Phys. B*, vol. 96, no. 2, pp. 345–353, 2009.
[17] T. Kaiser, D. Flamm, S. Schröter, and M. Duparré, "Complete modal decomposition for optical fibers using CGH-based correlation filters," *Opt. Express*, vol. 17, no. 11, p. 9347, 2009.
[18] D. Flamm, D. Naidoo, C. Schulze, A. Forbes, and M. Duparré, "Mode analysis with a spatial light modulator as a correlation filter," *Opt. Lett.*, vol. 37, no. 13, p. 2478, 2012.
[19] M. D. Gervaziev *et al.*, "Mode decomposition of multimode optical fiber beams by phase-only spatial light modulator," *Laser Phys. Lett.*, vol. 18, no. 1, p. 15101, 2020.
[20] D. Flamm, C. Schulze, D. Naidoo, S. Schröter, A. Forbes, and M. Duparré, "All-Digital Holographic Tool for Mode Excitation and Analysis in Optical Fibers," *J. Light. Technol.*, vol. 31, no. 7, pp. 1023–1032, 2013.
[21] J. Pinnell, I. Nape, B. Sephton, M. A. Cox, V. Rodríguez-Fajardo, and A. Forbes, "Modal analysis of structured light with spatial light modulators: a practical tutorial," *JOSA A*, vol. 37, no. 11, pp. C146–C160, 2020.
[22] J.-A. Valles, D. Benedicto, A. Dias, J. C. Martin, and J. Solis, "Characterization of multicore integrated active waveguides written in an Er3+/Yb3+ codoped phosphate glass," *J. Light. Technol.*, 2021.
[23] J. W. Goodman, "Introduction to Fourier optics. 2005," *Roberts Co. Publ.*, 2008.
[24] W. Ren, Z. Tan, and G. Ren, "Analytical formulation of supermodes in multicore fibers with hexagonally distributed cores," *IEEE Photonics J.*, vol. 7, no. 1, pp. 1–11, 2015.
[25] A. Ghatak and K. Thyagarajan, *An introduction to fiber optics*. Cambridge: Cambridge university press, 1998.
[26] W. H. Lee, "Sampled Fourier Transform Hologram Generated by Computer," *Appl. Opt.*, vol. 9, no. 3, pp. 639–643, 1970.

[27] C. B. Burckhardt, "A simplification of Lee's method of generating holograms by computer," *Appl. Opt.*, vol. 9, no. 8, p. 1949, 1970.
[28] C. K. Hsueh and A. A. Sawchuk, "Computer-generated double-phase holograms," *Appl. Opt.*, vol. 17, no. 24, pp. 3874–3883, 1978.
[29] V. Arrizón and D. Sánchez-de-la-Llave, "Double-phase holograms implemented with phase-only spatial light modulators: performance evaluation and improvement," *Appl. Opt.*, vol. 41, no. 17, p. 3436, 2002.
[30] Holoeye, "LUNA Phase Only Spatial Light Modulator." [Online]. Available: https://holoeye.com/luna-phase-only-spatial-light-modulator/.
[31] S. Reichelt, "Spatially resolved phase-response calibration of liquid-crystal-based spatial light modulators," *Appl. Opt.*, vol. 52, no. 12, p. 2610, 2013.